IMAGE TRANSMISSION USING DS-SS COMMUNICATION SYSTEM WITH ADAPTIVE CFAR DETECTORS

Kazim Nanji, Joseph El Ghoul, Mohamed El-Tarhuni, and Mourad Barkat
Department of Electrical Engineering, American University of Sharjah, P. O. Box 26666, UAE

***Abstract* — In this paper, an experimental setup for transmitting images using a direct-sequence spread spectrum wireless communication system with various adaptive Constant False Alarm Rate (CFAR) detectors is presented. Images are sent at a chip rate of 12.5 MHz operating at 2.4 GHz carrier over a wireless indoor channel. Different CFAR detectors such as CA-CFAR, SO-CFAR, GO-CFAR, OS-CFAR and TM-CFAR are tested. It is shown that the TM-CFAR provides the best performance since it was able to detect all the paths available in the received signals and hence provides for greater multipath diversity compared to conventional constant threshold detectors. The OS-CFAR has the next best performance followed by the SO-CFAR and last the CA-CFAR. This is attributed to the non-homogenous environment due to multipath signals.**

***Index Terms* — Direct-Sequence Spread Spectrum, Constant False Alarm Rate, Image Transmission, Experimental Results**

I. INTRODUCTION

In wideband communication systems, such as Direct Sequence Spread Spectrum (DS-SS), the spectrum of the signal is spread over a large bandwidth. Typically, the signal bandwidth is much greater than the coherence bandwidth of the channel which results in frequency selective multipath fading [1]. In order to exploit system characteristics and achieve diversification in the received signal, the receiver should optimally combine the energies of the incoming multipaths. Since multipaths undergo independent fading, the optimal recollection of energies would enhance the received signal's reliability. Thus, efficient multipath detection scheme is needed to identify the desired multipaths in the given environment.

Therefore, one of the critical tasks of the receiver is the detection of the multipath components. It is desirable to have a detection scheme which maximizes the joint probability of detecting all incoming multipaths. It is also desirable not to detect undesirable signal as a multipath; i.e. minimize the probability of false alarm. In a conventional multipath detection schemes, the received signal energy at different delays is compared with a pre-defined fixed threshold value. If the energy exceeds the threshold, then the presence of a desired multipath at a particular delay is declared. The selection of the threshold is important in determining both probabilities of detection and false alarm.

Fixed threshold selection however is suboptimal because a slight increase in noise and interference power, as compared to signal power, would result in a large increase in the probability of false alarm and a degrade in the receiver's performance. Thus, adaptive threshold techniques are needed to maintain a constant false alarm rate (CFAR) [1].

Some work on adaptive threshold detection applied to Direct Sequence Spread Spectrum (DS-SS) started appearing in the literature during the last few years [4]-[6]. In [5], an adaptive serial search system of pseudo-noise (PN) sequences for DS-SS systems in multipath Rayleigh fading channels was considered. It was observed, from the simulation results, that the OS-CFAR processor outperforms the CA-CFAR processor in the presence of multiple-access interferences. It was also observed in [6] that the ordered statistics acquisition processor (OSAP) is robust in multipath situations, while the mean level acquisition processor (MLAP) masks some multipath components.

To date, there is little experimental work published on using CFAR detectors for DS-SS systems. Most investigations previously presented use computer simulation or analytical tools to assess the performance of such systems. It is the objective of this paper to provide experimental results to compare the performance of different CFAR detectors over realistic wireless channel conditions. This paper is organized as follows: the signal model and the adaptive CFAR detectors are described in Section II. Section III explains the experimental setup and Section IV presents the results. Finally, Section V presents the conclusions.

II. SIGNAL MODEL AND ADAPTIVE CFAR DETECTORS

Consider the transmission of a wideband direct-sequence spread spectrum signal over an indoor wireless channel. The transmitted baseband signal is modeled as

$$x(t) = \sqrt{P} \sum_{m=0}^{M-1} \sum_{k=0}^{K-1} b_m c_k \, g(t - mT_b - kT_c) \qquad (1)$$

where P is the transmitted signal power, $b_m \in \pm 1$ is the mth information bit, $c_k \in \pm 1$ is the kth chip in the spreading code, $g(t)$ is the pulse shape. The number of data bits per frame is M; the number of chips per bit is K, T_b is the bit duration and T_c is the chip duration.

The received signal through the multipath channel is given by

$$r(t) = \sum_{l=0}^{L-1} \alpha_l x(t - \tau_l) + w(t) \qquad (2)$$

where α_l and τ_l are the complex channel gain and delay offset for the l[th] path, respectively. The total number of paths is L. It is assumed that α_l is modeled as a complex Gaussian random variable with zero-mean (no line of sight) or non zero-mean (line of sight) cases. The delay offset is assumed to be uniformly distributed over one spreading code period (KT_c). The background noise $w(t)$ is modeled as an additive white Gaussian noise (AWGN) process.

The system considered in this paper utilizes the received signal to provide accurate estimates of the multipath delays, $\hat{\tau}_l$, so that a RAKE receiver may be used to collect all the energy in the multipath signals. The received baseband signal is sampled at a rate of N_s / T_c so we have N_s samples per chip. The samples are applied to a chip matched filter and the filter output is used to estimate the energy in every possible delay offset with a resolution (step size Δ) of 1/2 chip by correlating the filter output with different replica of the spreading code.

The correlator output during the n[th] bit interval for the q[th] delay offset is given by

$$X_q(n) = \left| \sum_{k=0}^{K-1} r_m(k-q)c(k) \right|^2 \qquad (3)$$

for $q = 0,1,2,..., M/\Delta - 1$. The energy obtained for the same offset is accumulated over several data blocks to provide better averaging for the noise and stronger signal energy.

Conventional multipath detection schemes use the parameter in (3) to provide delay estimates by finding the offsets that have the strongest values. A threshold is set so that any value that exceeds the threshold is considered as multipath component. In this paper, we discuss other ways of setting this threshold based on adaptive constant false alarm criterion as discussed below.

Setting the threshold is a challenging task since having a high threshold will result in missing some of the paths while using a low threshold value will result in noise spikes accepted as correct paths (false alarm). The main idea of CFAR is to select the threshold such that the false alarm rate is kept at a constant acceptable level. This requires the use of a variable threshold that is adjusted according to the noise power in the received signal. Thus, an estimate of the noise power should be obtained from the correlation results in (3).

A typical CFAR detector is shown in Fig. 1. The output of the square law detector is fed into a tapped delay line of length N in order to estimate the noise power from the reference cells (excluding the cell under test). To avoid any signal energy spill from the test cell into directly adjacent cells, which may affect the noise power estimate, the adjacent cells (guard cells) are completely ignored.

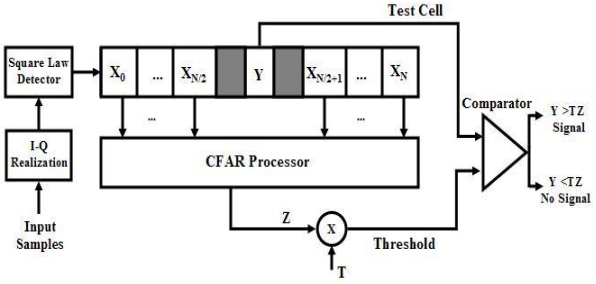

Fig. 1. CFAR detector

Each cell is tested separately and we assume that the cell under test is the one in the middle. The statistics of the reference windows are obtained from the $N/2$ leading cells and $N/2$ lagging cells, respectively. Thus, a total of N noise samples are used to estimate the background environment noise level Z. The noise level Z is then multiplied by a scaling factor called the threshold multiplier T which is a function of the probability of false alarm P_f and the window length N. The product TZ is the resulting adaptive threshold which is compared to the test cell and a decision is made to whether this cell is a multipath component or just noise.

The origins of CFAR goes back to the work presented in [3] where the cell averaging (CA)-CFAR detector was presented. In CA-CFAR, the threshold used to test the target cell (or delay offset) is calculated based on the average of all reference cells. It has been shown that the CA-CFAR detector is optimum in homogeneous background in the sense that it achieves a detection probability that approaches that of the (ideal) Neyman-Pearson detector as the number of reference cells becomes infinite. On the other hand, the CA-CFAR detector suffers from severe performance degradation in the presence of interfering signals or multipath in its reference window, or when the test cell is in a non-homogenous environment.

The CA-CFAR detector estimates the noise level by simply averaging all the reference cells

$$Z = \sum_{i=1}^{N} X_i \qquad (4)$$

In order to adapt to non-homogeneous environments, many alternative CFAR detectors have been proposed. The smallest–of (SO) CFAR, which can offer better performance in a multiple target environment, obtains its background noise estimate by choosing the smallest $N/2$ noise samples representing either the leading or lagging window [8]. Another CFAR detector proposed in non-homogenous background is the greatest–of (GO) CFAR, which obtains its background noise estimate by choosing the largest $N/2$ noise samples representing either the leading or lagging window. The GO-CFAR is capable of

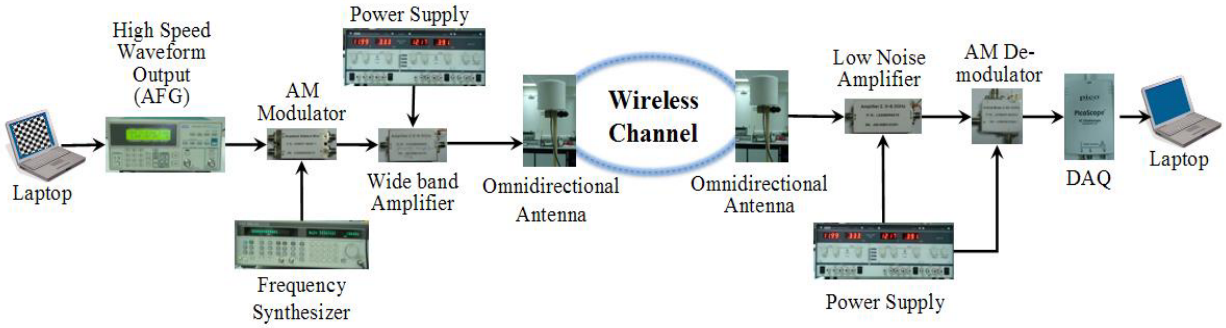

Fig 2. Experimental setup

minimizing the false alarm rate in case of a clutter edge [9].

Another CFAR detector based on ordered statistics (OS) was proposed in [4]. In the OS-CFAR detector, the cells are ranked in ascending order according to their magnitude and the detector chooses one ordered sample to represent the noise level estimate in the cell under test. This detector possesses a good ability to counter multipath and performs better in a non-homogenous background noise. Even though the OS-CFAR detector has a small additional detection loss over the CA-CFAR detector in homogeneous backgrounds, it can resolve closely spaced interferences.

The OS-CFAR detector involves a sort routine in which the cells are rank-ordered to yield

$$X_{(0)} \le X_{(1)} \ldots \le X_{(k)} \le \ldots \le X_{(N-1)} \le X_{(N)} . \qquad (5)$$

The k[th] largest cell chosen to estimate the noise level is

$$Z = X_{(k)} \qquad (6)$$

where k equals $3N/4$ [4].

As for the trimmed mean (TM) detector, the TM-CFAR detector involves a sort routine, similar to the OS-CFAR, and trims T_1 and T_2 cells from both the leading and lagging windows respectively, and then averaging the remaining cells to get the noise background estimate Z

$$Z = \sum_{i=T_1+1}^{N-T_1-T_2} X_i . \qquad (7)$$

The expressions for the probability of detection, probability of false alarm, and the threshold multiplier for each of the CFAR detectors discussed above is presented in [7].

III. Experimental Setup

The block diagram of the experimental wideband DS-SS system is shown in Fig 2. The transmitted waveform is generated in MATLAB and is composed of a PN code, generated by simulating a 6-bit register, modulated by the bits representing the image to be transmitted. The transmitter is composed of a high speed Arbitrary Function Generator (AFG) running at a chip rate of 12.5 Mcps. The laptop is connected to the AFG through a USB-to-GPIB cable to store the waveform in one of USER memory sets. The output of the AFG and output of frequency synthesizer is applied to an amplitude modulator component. The carrier frequency is set to 2.4 GHz. The RF wideband signal is applied to a wideband power amplifier and transmitted through an Omni-directional antenna.

The signal travels through the indoor wireless channel to the receiver located 3-4 meters from the transmitter such that there was line of sight. The measurements were conducted inside a Lab as illustrated in Fig. 3. The locations of the transmitter and the receiver are labeled in the sketch.

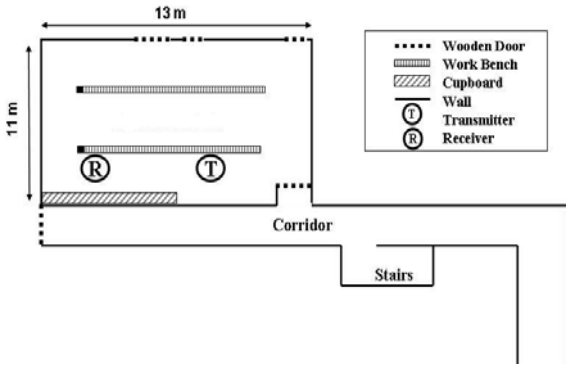

Fig. 3. Lab layout.

The signal is received using a wideband Omni-directional antenna, passed through a low noise amplifier, demodulated with a coherent detector, and finally the baseband signal is applied to data acquisition system (Pico Scope receiver) with a sampling rate of 50 Msps. The sampled signal is further processed using MATLAB code in order to obtain the energy profile of the received signal as a function of time delay offset. The process involves PN code generation, matched filtering, and calculating correlation between the received signal and delayed versions of the PN code. Thereafter, the energy profile is utilized for adaptive CFAR detection of multipaths, and ultimately, the detected delays are used to de-spread the received signal to obtain bits representing the image.

IV. RESULTS

To demonstrate the quality of image transmission for different CFAR detectors, the image (digital-one) shown in Fig. 4 is used. Fig. 5 shows the energy profile measured, at location labeled R in Fig. 3, inside the lab. There are two evident peaks in this case, which represent the multipaths to be detected and used in RAKE receiver to combine the energies.

Fig. 4. Transmitted image; Digit-one

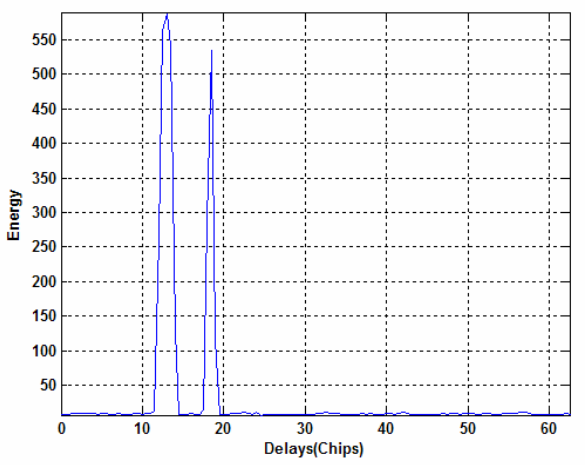

Fig. 5. Energy profile of Digit-one transmitted

The above observation was based on visual inspection of the energy profile to decide on how many paths are present in the channel and at which time delay. However, in practice we want the CFAR detector to make this decision. All the various CFAR detectors proposed in this paper were used with the real data energy profile above using different window sizes N. To avoid the problem of energy spill over adjacent cells, we have eliminated the CFAR decisions that declare the presence of consecutive paths (within two chips apart) since this is the maximum range that the PN autocorrelation function spans ($\pm T_c$). Thus, we consider that all the delay offsets falling within two chips correspond to one multipath component.

Upon transmission of the digit-one image, Fig. 6 shows the received image using various CFAR detectors of the same window length N with T_1=2 and T_2=4 for the TM-CFAR detector case. It is observed that the OS-CFAR and TM-CFAR detectors outperform the CA-CFAR and SO-CFAR detectors. On the other hand, Fig. 7 presents the case when the transmitted carrier power is decreased from 14 dBm to 10 dBm. It is observed that, for the same window length N, the TM-CFAR detector gives the best performance.

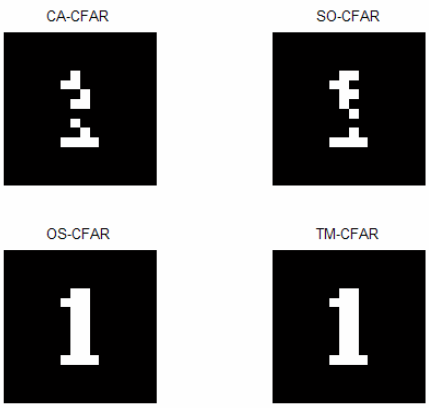

Fig. 6. Demodulated received image using various CFAR detectors having N=16; transmitted carrier power = 14 dBm

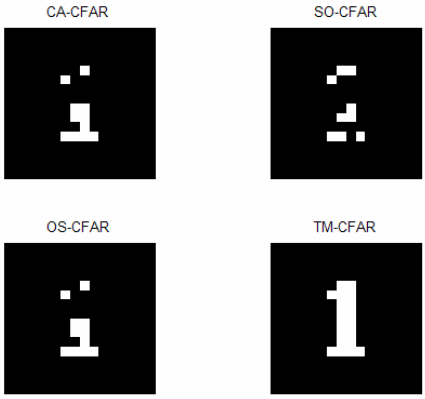

Fig. 7. Demodulated received image using various CFAR detectors having N=16; transmitted carrier power = 10 dBm

The results which were presented up till now reflected the combined result of all the paths, regardless of their accuracy, provided by the CFAR detector. Hereafter, the validity of each path detected by various CFAR detectors is explored and its impact on the final output is analyzed. As shown in Fig. 8, the CA-CFAR detector provides both correct and wrong paths (false alarms). It was also observed that if we provide a path to the receiver that corresponds to the spill over of a strong path, then we obtain an image having a high similarity to the transmitted image, but embedded with noise.

The paths provided by the various CFAR detectors are shown in Table 1. When these paths are used to de-spread the received signal individually, the corresponding output images are shown in Fig. 9. It is observed that the GO-CFAR detected fewer paths compared to other CFAR detectors, but did not generate a single false alarm. On the other hand, the SO-CFAR detected four paths out of which only one is a correct path. As for the CA-CFAR detector, it was able to detect the two paths with the high energy level out of which one bears no information. In contrast, the OS-CFAR and the TM-CFAR were able to detect the two paths with high energy level, in addition to two closely spaced paths occurring at chip delays 13 and

14 – just 1 chip apart. Apparently, the path occurring at chip delay=18.5 is a false path despite its high energy level.

V. CONCLUSIONS

In this paper, various adaptive CFAR algorithms were implemented on real data obtained from an experimental indoor wideband DS-SS communication system that performs image transmission. Energy profiles at different locations were obtained. The CFAR detectors are compared based on the ability of correctly detecting the existing multipath components. It is shown that the TM-CFAR and OS-CFAR detectors outperform the conventional CA-CFAR, SO-CFAR, and GO-CFAR detectors in terms of accurate detection of multipaths.

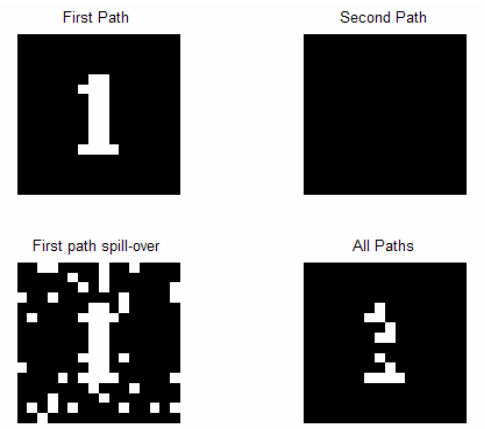

Fig. 8. Demodulated received image using different paths provided by the CA-CFAR detector with N=24

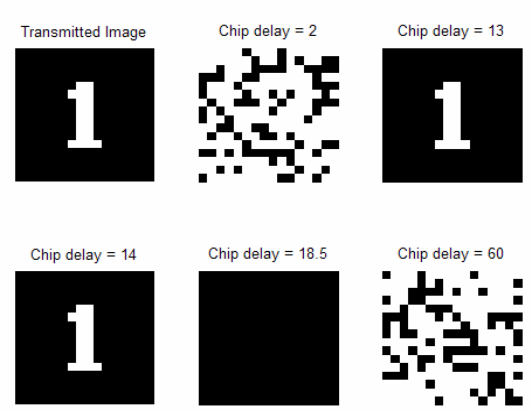

Fig. 9. Demodulated received image at different chip delays for the Digit-one transmitted image

REFERENCES

[1] T. Rappaport, *"Wireless Communications: Principles and Practice"*, 2nd ed., Prentics Hall, New Jersey, 2001.

[2] M. Barkat, "*Signal Detection and Estimation*", 2nd ed., Artech House, Boston, 2005.

[3] H.M. Finn, and R. S. Johnson, "Adaptive Detection Mode with Threshold Control as a Function of Spatially Sampled Clutter-Level Estimates," *RCA Review*, Vol. 29, pp. 414-464, September 1968.

[4] H. Rohling, "Radar CFAR Thresholding in Clutter and Multiple Target Situations," *IEEE Trans. on Aerospace and Electronic Systems,* Vol. AES-19, No. 4, pp. 608-621, 1983.

[5] S. Benkrinah and M. Barkat, "An Adaptive Code Acquisition Using Order Statistic-CFAR in DS/CDMA Serial Search for a Multipath Rayleigh Fading Channel," *Third IEEE International Conference on Systems, Signals and Devices*, Tunisia, March 2005.

[6] C. J. Kim, H. J. Lee, and H. S. Lee, "Adaptive Acquisition of PN Sequences for DSSS Communications," *IEEE Trans. on Communications*, Volume 46, No. 8, pp. 993-996, August 1998.

[7] P. P. Gandhi and S. A. Kassam, "Analysis of CFAR Processors in Nonhomogeneous Background," *IEEE Transactions on Aerospace and Electronic Systems,* Vol. AES-24, No. 4, July 1988, pp. 427-445.

[8] G. V. Trunk, "Range resolution of targets using automatic detectors", *IEEE Transactions on Aerospace and Electronic Systems,* 14(5), September 1978, pp. 750-755.

[9] G. V. Hansen, J. H. Sawyers, "Detectability loss due to greatest-of selection in a cell averaging CFAR", *IEEE Transactions on Aerospace and Electronic Systems,* 16, 1980, pp. 115-118.

Table 1. Location of multipath provided by CFAR detectors

Detector	Chip Delays				
CA-CFAR	-	13	-	18.5	-
SO-CFAR	2	13	-	18.5	60
GO-CFAR	-	13	-	-	-
OS-CFAR	-	13	14	18.5	-
TM-CFAR	-	13	14	18.5	-